DR JOSE ANTONIO DIAZ (Orcid ID : 0000-0001-5205-2118)

Article type : Methodological Articles

A Cost-Effective Flexible Pre-Clinical Tool for Studying the Fibrinolytic System in Venous Thrombosis: An Update on The Electrolytic IVC Model (EIM)

Olivia R Palmer*[1], Maxim E Shaydakov†[1], Joshua P Rainey‡, Daniel A Lawrence§, Joan M Greve*, José A Diaz[3]

[1]These authors contributed equally to this work

*Department of Biomedical Engineering, University of Michigan, Ann Arbor, MI.

†Department of Surgery, UT Health San Antonio, San Antonio, TX.

‡Department of Surgery, Vascular Surgery, University of Michigan, Ann Arbor, MI.

§Department of Internal Medicine, University of Michigan, Ann Arbor, MI.

Correspondence to:

José Antonio Diaz
Research Assistant Professor
Department of Surgery, Vascular Surgery
Conrad Jobst Vascular Research Laboratories
North Campus Research Complex
2800 Plymouth Rd, Building 26, Room 251N
Ann Arbor, MI 48109, USA
josediaz@med.umich.edu

This is the author manuscript accepted for publication and has undergone full peer review but has not been through the copyediting, typesetting, pagination and proofreading process, which may lead to differences between this version and the Version of Record. Please cite this article as doi: 10.1002/rth2.12074

Part of this work was accepted and presented as a poster at the International Society for Thrombosis and Haemostasis 2017 Congress in Berlin (PB 089-Animal Models-Monday, July 10).

Word Count (Introduction through Discussion): 3456

Essentials

- Three key updates are provided on the electrolytic inferior vena cava model (EIM)
- The originally described stimulator equipment has been discontinued; we developed an alternative

- The fibrinolytic system and the current and time dependency of the EIM was characterized

- EIM allows the investigation of the fibrinolytic system, critical for endovascular therapies

Abstract

Background: The electrolytic inferior vena cava model (EIM) is a murine venous thrombosis (VT) model that produces a non-occlusive thrombus. The thrombus forms in the direction of blood flow, as observed in patients. The EIM is valuable for investigations of therapeutics due to the presence of continuous blood flow. However, the equipment used to induce thrombosis in the original model description was expensive and has since been discontinued. Further, the fibrinolytic system had not been previously studied in the EIM.

Objectives: We aimed to provide an equipment alternative. Additionally, we further characterized the model through mapping the current and time dependency of thrombus resolution dynamics, and investigated the fibrinolytic system from acute to chronic VT.

Results: A voltage to current converter powered by a direct current power supply was constructed and validated, providing an added benefit of significantly reducing costs. The current and time dependency of thrombus volume dynamics was assessed by MRI, demonstrating the flexibility of the EIM to investigate both pro-thrombotic and anti-thrombotic conditions. Additionally, the fibrinolytic system was characterized in EIM. Centripetal distribution of plasminogen was observed over time, with peak staining at day 6 post thrombus induction. Both active circulating plasminogen activator inhibitor-1 (PAI-1) and vein wall gene expression of PAI-1 peaked at day 2, coinciding with a relative decrease in tissue plasminogen activator and urokinase plasminogen activator.

Conclusions: The EIM is a valuable model of VT that can now be performed at low cost and may be beneficial in investigations of the fibrinolytic system.

Key Words

Animal Models, EIM, Electrolysis, Fibrinolysis, Magnetic Resonance Imaging, Veins, Venous Thromboembolism, Venous Thrombosis

Introduction

Animal models are critical to study the biology of venous thrombosis (VT). The electrolytic inferior vena cava model (EIM) was developed to simulate VT in the clinical scenario of a non-occlusive thrombus. By applying a small constant current to a copper wire inserted into the inferior vena cava (IVC), free radicals are released which activate endothelial cells and initiate the thrombotic process in the constant presence of blood flow. These conditions mimic the clinical scenario of a non-occlusive thrombus (**Fig. 1**)[1–3]. This method produces a thrombus that is highly consistent in size. The EIM has been used in the United States and beyond to study VT in both anti-thrombotic and pro-thrombotic conditions, demonstrating the flexibility of the model [4,5].

Since the initial development of the EIM in 2010, several changing circumstances have driven a need for an update on the model. First, the originally described stimulator equipment was expensive and has since been discontinued. Second, the dependence of thrombus size on current and time were assumed, but had not previously been demonstrated. Third, increasing interest in targeting the fibrinolytic system for treatment of VT and the results of the ATTRACT trial emphasize a need for basic science evidence on the fibrinolytic system of thrombi in the presence of blood flow [6,7]. The EIM provides a favorable environment for such therapeutic targets due to the sustained blood flow access to the thrombus. However, the fibrinolytic system had not previously been investigated in the EIM. In this communication, we addressed all three

of these important updates; we developed an equipment alternative to the previously described system, investigated the current and time dependency of thrombus size, and characterized the fibrinolytic system in the EIM.

Materials and Methods

Mice and EIM Surgical Procedure

All experiments were performed at the University of Michigan with approval from the University of Michigan's Institutional Animal Care and Use Committee (IACUC) and conducted in accordance with *The Guide for the Care and Use of Laboratory Animals* [8]. Male C57BL/6 mice aged 10-12 weeks were anesthetized with 2% isoflurane, placed in dorsal recumbency, and a midline laparotomy was performed. The IVC was exposed, any lateral branches were ligated using 7-0 Prolene suture (Ethicon, Inc., Somerville, NJ), and back branches remained patent. A 30-gauge silver coated copper wire (KY-30-1-GRN, Electrospec, Dover, NJ, USA) with exposed copper wire at the end was attached to a 25-gauge needle and inserted into the IVC and positioned against the anterior wall (anode). Another needle was implanted subcutaneously at the proximal end of the laparotomy incision, completing the circuit (cathode). A detailed video demonstrating the surgical technique is available [3].

A constant current of 250 μA was applied for 15 minutes for standard procedures [3]. To investigate the current and time dependency of the EIM, either the current or time was modified to 100 μA or 7.5 minutes, respectively. The current was supplied by either the previously described Grass S48 square wave stimulator and constant current unit (Grass Technologies, Astro-Med, Inc., West Warwick, RI), or by the voltage-to-current converter, described below (**Fig. 2**). The direct current results in the release of free radicals within the IVC, which in turn activate endothelial cells and initiate a thrombogenic environment in the constant presence of blood flow. The needle was then removed and the abdomen closed in two layers; the muscle and peritoneum was closed with 5-0 Vicryl (Ethicon, Inc., Somerville, NJ), the skin closed with Vetbond (3M, St. Paul, MN).

Mice not undergoing magnetic resonance imaging (MRI) were euthanized at specific time points post thrombosis in order to analyze thrombus weight and perform histology, PCR, or ELISA. True controls (TC), surgically naïve mice, were utilized for baseline molecular assays.

EIM Equipment

EIM was performed either with the previously described discontinued stimulator and constant current unit, or with a voltage to current converter (VIC), as pictured in **Fig. 2**. The AD620 operation amplifier may be used in conjunction with a second operational amplifier, such as the AD705 (DigiKey, Thief River Falls, MN). A 40 kΩ resistor (R1) was used with an input voltage of +5 and -5 volts, but the desired resistor and/or voltage may be calculated based on the input current as follows:

$$I_L = \frac{V_x}{R1} = \frac{[(V_{IN+}) - (V_{IN-})]G}{R1}$$

where I_L is the current applied to the load, typically 250 µA, R1 is the resistor used, V_{IN} is the positive and negative input voltage, and G is the gain. A gain resistor (R_G) is not needed for this application, so the gain (G) remains at 1. The circuit was powered by a DC power supply (Agilent E3630A, KeySight Technologies, Santa Rosa, CA). Prior to surgery, a sample load resistor (e.g. 100 Ω) was connected to the circuit and a multimeter was connected in series to fine tune the supplied voltage to deliver 250 µA (or desired current) to the load.

Validation and Characterization

In vivo validation of the VIC was performed by comparing thrombus weights at days 2, 6, and 11-post thrombus induction against thrombi produced using the stimulator and constant current unit. Following validation, the vein wall was isolated for qRT-PCR analysis, and 500 µL of blood was collected for circulating plasminogen activator inhibitor (PAI)-1 activity assay. EIM was performed in a separate group of mice for immunohistochemistry at the same time points.

Additionally, to investigate the current and time dependency of the EIM, thrombus was induced in three groups: standard, 250 µA for 15 min; reduced current, 100 µA for 15 min; and reduced

time, 250 µA for 7.5 min. Thrombus volume was followed over time using MRI, described below.

Thrombus Weight

At the time of euthanasia, the IVC and the associated thrombus were removed and weighed for wet thrombus weight. The IVC was separated from the aorta and surrounding tissue, and a segment from just below the left renal vein to the iliac bifurcation was removed for weighing. The lymph nodes were removed from the IVC prior to weighing. After determining thrombus weight, the vein wall was separated from the thrombus for subsequent assessment by qRT-PCR.

Thrombus Volume Assessment by MRI (in vivo)

The current and time dependency of the EIM was investigated in three groups of mice (standard, reduced current, or reduced time). Thrombus size was monitored *in vivo* by MRI at days 1, 2, 4, 6, 9, 11, and 14 following thrombus induction. Mice were anesthetized using 2% isoflurane and imaged supine on a preclinical 7 Tesla MRI scanner. Respiration was monitored with a respiratory pillow (SA Instruments, Inc., NY), and a PID controller was used to maintain the animal's temperature at 37±1ºC via warm air circulation through the bore of the magnet. To assess thrombus volume, 2D time-of-flight gradient echo axial slices were acquired from the renal vessels to the iliac vessels (18 contiguous slices, each 1 mm thick; repetition time 15 ms, echo time 4.9 ms, field of view 30 mm x 30 mm, flip angle 20º, matrix 256 x 256 zero-filled to 512 x 512, in-plane resolution 58.6 µm x 58.6 µm, number of excitations 3, imaging time 4 minutes). Thrombus volume was assessed by summing thrombus area in each axial slice (MRVision, Winchester, MA).

Quantitative Real-Time Polymerase Chain Reaction

Ribonucleic acid (RNA) was isolated from the IVC wall by homogenizing in TRIzol reagent (Invitrogen, Carlsbad, CA) per the manufacturer's protocol. Gene expression of PAI-1, tissue plasminogen activator (t-PA), and urokinase plasminogen activator (u-PA) were determined by

qRT-PCR using commercially available primers (mouse PAI-1: PPM03093C, mouse t-PA PPM03855B, mouse u-PA PPM03095D) and SYBR master mix (SA Bioscience, Frederick, MD) in a Rotor-Gene 3000 thermocycler (Corbett Life Science, San Francisco, CA), as previously described [9,10]. Gene expression was normalized to β-actin (mouse β-actin: PPM02945B) levels for each specimen.

Immunohistochemistry

Harvested IVC samples containing thrombus were formalin fixed for 2 hours, dehydrated in alcohol, paraffin embedded, and cut into 5 µm longitudinal sections. Nonspecific sites were blocked with normal serum, and sections were incubated with primary antibodies to Plasminogen (1:500, Genetex, Inc.; Catalog number GTX102877, Irvine, CA.) A species-specific ABC peroxidase kit (Vector Laboratories Inc., Burlingame, California) was used according to the manufacturer's instructions for the corresponding secondary antibody and subsequent steps. Color development was performed with diaminobenzidine (DAB). Mosaic images were created via light microscopy (Nikon, Tokyo, Japan) under 40x magnification and quantification of percent positive staining was performed as previously described [11].

PAI-1 Activity Assay

500 µL of blood was collected by cardiocentesis at harvest using a syringe with 0.05 mL of sodium citrate, and active and total PAI-1 was determined as previously described [12]. In brief, to measure active murine PAI-1 concentrations in plasma samples, human u-PA (rheotromb) was coupled to carboxylated beads (Luminex, Austin, TX) and used to capture active PAI-1. A standard curve was generated using known concentrations of murine PAI-1 in PAI-1 depleted mouse plasma (Molecular Innovations, Novi, MI). The assay was performed by adding 25 µL of either the standards or samples to a 96 well plate filter plate (Millipore, Billerica, MA). Each well then received 25 µL PBS-1% BSA and 5000 beads in 30 µL of PBS-1% BSA. The wells were incubated overnight in the dark at 4°C. The solution from each well was removed by vacuum suctioning and each well was washed twice with 200 µL PBS-0.05% Tween-20. The beads were mixed with continuous shaking in the dark at room temperature for 2 hours with 50

μL of 2μg/mL biotin-labeled rabbit anti-mouse PAI-1 (Molecular Innovations, Novi, MI). The wells were vacuum washed and 25 μL of 4 μg/mL streptavidin-R-phycoerythrin (Molecular Probes, Eugene, OR) was added to each well, and the mixture incubated in the dark with continuous agitation at room temperature for 30 minutes. Finally, the solution was removed from each well by vacuum suctioning, the beads were washed three times with 200 μL of PBS-0.05 % Tween-20, and 150 μL of sheath fluid was added for 5-10 minutes. The beads were then read with a Luminex 100 (Luminex, Austin, TX), median setting, 100 μL sample size, 100 events/bead.

Statistical Analysis

All statistical analyses were completed using GraphPad Prism 7 (GraphPad Software, San Diego, CA). Comparison of thrombus weight between the VIC and Grass S48 was performed using an unpaired t test with Welch's correction. A two-way ANOVA analysis using the Tukey's multiple comparison test was performed between VIC groups for the current and time dependency investigation as well as comparison of immunohistological plasminogen expression between time points. Relative expression of t-PA, u-PA, and PAI-1 in the vein wall as well as active circulating PAI-1 was compared to true controls for each time point using two-way ANOVA with Dunnett's multiple comparison test. A p value of ≤ 0.05 was considered significant. Data was reported as mean ± standard error of the mean (SEM).

Results

Voltage-to-current circuit provides cost-effective system for performing EIM

We constructed a voltage-to-current converter (VIC) powered by a common DC power supply to offer an equipment alternative to perform the EIM. The development of the VIC provided an added benefit of a significant cost reduction (**Table 1**). *In vivo* validation of the VIC was performed by comparing thrombus size by wet weight at days 2, 6, and 11 post thrombus induction to thrombi produced using the Grass S48. Thrombus weights were not significantly different between the VIC and Grass S48 at any of the time points studied (**Fig. 2**).

Thrombus Size in EIM is both Current and Time Dependent

The dependence of thrombus size on the supplied current and duration of application in the EIM was assessed by MRI from day 1 to 14 post-thrombosis to enable tracking of thrombus size (via volume) in the same mouse over time. Time-of-flight imaging confirmed continuous blood flow at peak thrombus size, day 2 post-thrombus initiation (**Fig. 3**). Reduction of either current or time resulted in significantly smaller thrombus volume at all time points compared to standards (at day 2: 20.5±1.3 mm^3 standard vs. 5.88±0.7 mm^3 reduced current vs. 5.93±0.6 mm^3 reduced time, $p<0.05$) (**Fig. 3**). Interestingly, no statistical differences were found between the two modified groups. Importantly, thrombus size within each group was highly consistent between mice (coefficient of variation at day 2: controls 11%, reduced current 20%, reduced time 19%).

The Fibrinolytic System is Suppressed in Acute VT

The fibrinolytic system was investigated in the EIM at days 2, 6, and 11. Qualitatively, positive immunostaining for plasminogen was initially found along the perimeter day 2, with distribution throughout the thrombus at days 6 and 11. Maximum staining was measured at day 6 (**Fig. 4**). Active circulating PAI-1 was significantly increased compared to true controls at days 2 and 11, with peak concentration at day 2 post thrombus induction (day 2: 2764±120 pg/mL, day 11: 1775±292 pg/mL vs. controls: 1063±140 pg/mL, $p<0.05$) (**Fig. 5**). Interestingly, active circulating PAI-1 at day 6 was not different from true controls, indicating a dynamic process of thrombus burden with changing thrombus composition. PAI-1 expression in the IVC wall paralleled active circulating PAI-1 expression (**Fig. 5**). Vein wall PAI-1 expression peaked at day 2, with a down-regulation trend of t-PA and u-PA at the same time point (p=NS). The opposite PAI-1 to t-PA and u-PA relationship was observed at day 11 (**Fig. 5**).

Discussion

Animal models provide critical insight to understanding the mechanisms of VT. However, there is no single model that can replicate the complexities of deep vein thrombosis. Moreover, model

selection should be driven by the specific research question. Thus, a deep understanding of each available animal model including detailed characterization is necessary for choosing the appropriate model for a given research question. The EIM is the only currently available mouse model that provides both thrombus size consistency and maintained blood flow in the IVC and around the thrombus independently of the time point investigated, which is favorable for systemically administered therapeutic investigations.

The EIM was originally described using a stimulator and constant current unit from Grass Technologies to follow the procedures used by Luchessi and collaborators [13] in their canine coronary artery thrombosis model. This equipment was expensive and has since been discontinued. Alternative compatible stimulator and constant current units are difficult to find, but products from a Japanese company Nihon Kohden have been used [5]. This equipment also can be expensive, amounting to several thousands of dollars (**Table 1**). Thus, the high cost and discontinuation of the originally described equipment warranted an update to improve accessibility and characterization of the EIM.

Induction of thrombosis in EIM is accomplished by application of a very small constant current. In the original model description, this was regulated by the constant current unit (CCU1, Grass Technologies), which was powered by a compatible stimulator providing a very high voltage (150 V). The unit required this high voltage input to achieve accuracy in delivering 250 µA. Alternative current sources, however, do not require high voltage sources, eliminating the need for a high-voltage stimulator. Other constant current sources sold typically do not provide a range sufficiently low for this application. We chose to implement an operational amplifier constant current source for cost effectiveness, which we powered with a common DC power supply that many labs will have readily available. The VIC was validated on the bench using a multimeter and *in vivo* by comparing thrombus weight at days 2, 6 and 11, yielding results that were not statistically different from the stimulator and constant current unit. Thus, the model may be implemented at costs comparable to other murine models which only require a surgical scope and anesthesia machine.

Recently, a Japanese group presented a modification to the original EIM description to study a pro-thrombotic phenotype [5]. Typically, maximum thrombus burden is observed at day 2 with a thrombus-to-lumen ratio of 3:1 making this method very suitable to study "thrombus reduction", an attractive option when it comes to drug development and testing the potential role of pharmaceutical compounds for VT. Banno et al. adapted the original EIM by modifying the time (10 minutes instead of 15 minutes) and the current (200 µA instead of 250 µA), resulting in a smaller initial thrombus size for control mice, allowing them adequate sensitivity to detect larger thrombi in pro-coagulant mice. Their modification relied on the current and time dependency of the model, but also opened the question of how individual modifications of these variables would influence the dynamics of thrombogenesis and resolution.

Taking advantage of MRI to follow each mouse over time, we performed EIM with the original descriptive technique and in two experimental groups—one with a reduced current of 100 µA and one with reduced time to 7.5 minutes. The results of this experiment demonstrated thrombus size in this model is current and time dependent, and that these modifications still produce highly consistent thrombus size. These results corroborate the flexibility of the EIM to fine tune the model to a desired thrombus size for a specific research question. Of note, modifications served to decrease either current or time rather than increase. This is because in our experience with the development of this methodology, we concluded that 250 µA was the highest safe current without inducing off-target pathology (we observed lower limb paralysis with currents beyond 250 µA, independent of the time of application; observational data).

The recently completed ATTRACT trial investigated the impact of prompt thrombus removal via pharmacomechanical catheter directed thrombolysis (PCDT) on post thrombotic syndrome [14]. PCDT involves both mechanical and chemical lysing of the thrombus from a catheter-based device embedded within the thrombus. Currently, there are no fibrinolytic drugs with FDA approval for the treatment of VT [15]. However, the use of t-PA as a chemical lysing agent is commonly used in endovascular procedures ("off-label" use). Its mechanism of action is conversion of plasminogen into plasmin, which breaks down fibrin. Thus, studying plasminogen content in this VT model provides a platform for further investigations from both a biological and therapeutic perspective. The continuous blood flow channel in the EIM at all time points

provides the possibility of direct drug access to the thrombus, even with systemically delivered therapies. However, before we move to therapeutics, the fibrinolytic system should be characterized in each animal model, as we did for this methodology (EIM). Our experiments addressed plasminogen concentration at different time points, gene expression of markers of the fibrinolytic system (PAI-1, u-PA and t-PA) in the vein wall directly in the area where the thrombus occurred, and active circulating PAI-1.

Plasminogen, the inactive precursor of the enzyme plasmin which degrades fibrin, is activated by t-PA and u-PA. Interestingly, the immunohistochemistry for plasminogen showed higher total concentrations at day 6, with plasminogen arranged from the thrombus perimeter (day 2) towards the center of the thrombus over time. This centripetal integration suggests that blood flow access to the thrombus may play an important role in the fibrinolytic process. Understanding plasminogen dynamics may provide basic science insights that could lead to a better understanding of therapeutic efficacy at different stages of VT.

PAI-1, one of the key inhibitors of t-PA and u-PA, was measured by gene expression in the vein wall and in its active circulating form. Total circulating PAI-1 correlated with PAI-1 gene expression in the vein wall, and interestingly, the peak of PAI-1 was observed at day 2, coinciding with the decreased expression of t-PA and u-PA. Taken together, this information supports that there is an impairment of the fibrinolytic system activity at day 2 (acute VT) favoring the development of a thrombus. This is aligned with previous work demonstrating that PAI-1 levels peaked at day 2 in the total IVC ligation model, which is considered a blood stasis model [12]. The impairment of the fibrinolytic system during acute VT suggests that VT is not only attributable to coagulation processes, but also a decrease in the fibrinolytic system, regardless of blood flow conditions. This insight not only improves our knowledge of the model but also increases our understanding of VT and is aligned with previous human VT publications [16].

In conclusion, we have demonstrated that the EIM can be performed using a VIC with the added benefit of reduced cost. Thrombus size in the EIM is both current and time dependent. We characterized the dynamics of thrombus resolution in reduced current and time of application

experiments, further confirming the flexibility of this model to study both anti-thrombotic and pro-thrombotic conditions. Regardless of the current and time of application used, this model generates thrombi that are highly consistent in size, as was demonstrated previously with thrombus weight and ultrasound [2], and now by MRI. Additionally, the EIM can be used to investigate the fibrinolytic system under flow conditions. The functionality of the fibrinolytic system increases over time as t-PA and u-PA are up-regulated and plasminogen disseminates throughout the thrombus, providing insights for improving future therapeutic approaches. Hence, the EIM provides a cost-effective, flexible pre-clinical tool for studying the fibrinolytic system in venous thrombosis.

Conflict-of-interest Disclosure

Jose Antonio Diaz, MD is on the Board of Directors of the American Venous Forum, as a Research Council Chair.

Acknowledgements

The authors would like to acknowledge Dennis Clafflin and Paige Castle for their guidance on the electronics of the VIC.

Authorship Contributions

OR Palmer, ME Shaydakov, and JA Diaz conceived and designed the study; OR Palmer, ME Shaydakov and JA Diaz performed surgeries; OR Palmer, ME Shaydakov, and JP Rainey collected and analyzed data; OR Palmer performed statistical analysis; OR Palmer, DA Lawrence and JA Diaz interpreted that data; OR Palmer, ME Shaydakov, and JA Diaz wrote the paper; OR Palmer, ME Shaydakov, DA Lawrence, JM Greve, and JA Diaz critically revised the paper; all authors gave final approval of the paper.

Figure Captions

Figure 1. A) Schematic representation of the EIM. Any lateral branches draining into the IVC distal to the left renal vein are ligated, and a 250 μA current is applied to a copper wire placed

within the IVC against the anterior wall. The right lymph node, consistently located near the bifurcation, serves as an anatomical reference for placement of the 25-gauge needle containing the copper wire. B) Gross anatomy images of the thrombus and vein wall at day 2 harvest; line markings denote mm. References: EIM – electrolytic inferior vena cava model, IVC – inferior vena cava.

Figure 2. The EIM was developed using a square wave stimulator and constant current unit (C, Grass Technologies), both of which are discontinued. Construction of a standard voltage-to-current converter (VIC) – circuit diagram shown in A and constructed circuit with standard DC power supply shown in B – provide a cost-effective alternative. The VIC was validated on the benchtop and then *in vivo* by thrombus weights at days 2, 6, and 11 to the Grass S48 system (n=5 per group, mean ± SEM, D). References: EIM – electrolytic inferior vena cava model, VIC – voltage to current converter, DC – direct current, NS – not statistically significant.

Figure 3. A) Contiguous axial MR images were used to quantify thrombus volume. Axial sections at the approximate midpoint of the thrombus at day 2 are shown for each group. Blood flow is visible surrounding the thrombus in all groups. The IVC is outlined in blue, the thrombus in green, and the aorta in red. Schematic representation of the thrombus is shown to the right of the MR images to highlight the thrombus size at day 2. B) Modifications to the model demonstrate the current and time dependency of thrombus size (n=3 per group, mean ± SEM) in the EIM, as measured by MRI. Time points were compared across groups, *$p<0.05$. References: MR(I) – magnetic resonance imaging, IVC – inferior vena cava.

Figure 4. A) Representative composite longitudinal images of thrombus stained for plasminogen at days 2, 6, and 11 post thrombus induction. B) Analysis for positive staining as a percentage of total thrombus area.

Figure 5. Dynamics of fibrinolytic system markers tissue plasminogen activator (t-PA), urokinase plasminogen activator (u-PA), and plasminogen activator inhibitor 1 (PAI-1) from the vein wall were assessed by qRT-PCR (left axis). Active circulating PAI-1 was assessed by ELISA (right axis). Data presented as mean ± SEM. TC – true controls (naïve animals).

References: TC – true control (surgically naïve mice), qRT-PCR – quantitative real time polymerase chain reaction.

Table Legends

Table 1. Equipment required and price ranges for the previously described system compared to the VIC. Sample product numbers are provided for each component for reference. References: VIC – voltage to current converter.

References

[1] Diaz JA, Hawley AE, Alvarado CM, Berguer AM, Baker NK, Wrobleski SK, Wakefield TW, Lucchesi BR, Myers DD. Thrombogenesis with continuous blood flow in the inferior vena cava. A novel mouse model. Thromb Haemost 2010;104:366–75. doi:10.1160/TH09-09-0672.

[2] Diaz JA, Alvarado CM, Wrobleski SK, Slack DW, Hawley AE, Farris DM, Henke PK, Wakefield TW, Myers DD. The electrolytic inferior vena cava model (EIM) to study thrombogenesis and thrombus resolution with continuous blood flow in the mouse. Thromb Haemost 2013;109:1158–69. doi:10.1160/TH12-09-0711.

[3] Diaz JA, Wrobleski SK, Hawley AE, Lucchesi BR, Wakefield TW, Myers DD. Electrolytic inferior vena cava model (EIM) of venous thrombosis. J Vis Exp 2011:e2737. doi:10.3791/2737.

[4] Diaz JA. Animal models of VT: to change or not to change? Blood 2015;126:2177–8. doi:10.1182/blood-2015-08-664011.

[5] Banno F, Kita T, Fernández JA, Yanamoto H, Tashima Y, Kokame K, Griffin JH, Miyata T. Exacerbated venous thromboembolism in mice carrying a protein S K196E mutation. Blood 2015;126:2247–53.

[6] Sugimoto K, Hofmann L V., Razavi MK, Kee ST, Sze DY, Dake MD, Semba CP. The safety, efficacy, and pharmacoeconomics of low-dose alteplase compared with urokinase for catheter-directed thrombolysis of arterial and venous occlusions. J Vasc Surg 2003;37:512–7. doi:10.1067/mva.2003.41.

[7] Lin M, Hsieh JCF, Hanif M, McDaniel A, Chew DK. Evaluation of thrombolysis using tissue plasminogen activator in lower extremity deep venous thrombosis with concomitant femoral-popliteal venous segment involvement. J Vasc Surg Venous Lymphat Disord 2017;5:613–20. doi:10.1016/j.jvsv.2017.04.018.

[8] Garber JC, Barbee RW, Bielitzki JT, Clayton LA, Donovan JC, Hendriksen CFM, Kohn DF, Lipman NS, Locke PA, Melcher J, Quimby FW, Turner P V, Wood GA, Wurbel H. Guide for the Care and Use of Laboratory Animals. 8th ed. National Academies Press (US); 2011. doi:10.17226/12910.

[9] Wojcik BM, Wrobleski SK, Hawley AE, Wakefield TW, Myers DD, Diaz JA. Interleukin-6: a potential target for post-thrombotic syndrome. Ann Vasc Surg 2011;25:229–39. doi:10.1016/j.avsg.2010.09.003.

[10] Patterson KA, Zhang X, Wrobleski SK, Hawley AE, Lawrence DA, Wakefield TW, Myers DD, Diaz JA. Rosuvastatin reduced deep vein thrombosis in ApoE gene deleted mice with hyperlipidemia through non-lipid lowering effects. Thromb Res 2013;131:268–76. doi:10.1016/j.thromres.2012.12.006.

[11] Lynch S, Figueroa CA, Diaz J, Jones L, Ikram M, Smith A, Saha P. Semiautomatic Computational Method for the Quantification of Histologic Elements of Experimental Venous Thrombi. J Vasc Surg Venous Lymphat Disord 2017;5:146–7. doi:10.1016/j.jvsv.2016.10.014.

[12] Diaz JA, Ballard-Lipka NE, Farris DM, Hawley AE, Wrobleski SK, Myers DD, Henke PK, Lawrence DA, Wakefield TW. Impaired fibrinolytic system in ApoE gene-deleted mice with hyperlipidemia augments deep vein thrombosis. J Vasc Surg 2012;55:815–22. doi:10.1016/j.jvs.2011.08.038.

[13] Romson JL, Haack DW, Lucchesi BR. Electrical induction of coronary artery thrombosis in the ambulatory canine: a model for in vivo evaluation of anti-thrombotic agents. Thromb Res 1980;17:841–53.

[14] Vedantham S, Goldhaber SZ, Kahn SR, Julian J, Magnuson E, Jaff MR, Murphy TP, Cohen DJ, Comerota AJ, Gornik HL, Razavi MK, Lewis L, Kearon C. Rationale and design of the ATTRACT Study: A multicenter randomized trial to evaluate pharmacomechanical catheter-directed thrombolysis for the prevention of postthrombotic syndrome in patients with proximal deep vein thrombosis. Am Heart J 2013;165:523–

530.e3. doi:10.1016/j.ahj.2013.01.024.

[15] Vedantham S. Catheter-directed thrombolysis to avoid late consequences of acute deep vein thrombosis. Thromb Res 2017. doi:10.1016/j.thromres.2017.08.010.

[16] Meissner MH, Zierler BK, Bergelin RO, Chandler WL, Strandness DE. Coagulation, fibrinolysis, and recanalization after acute deep venous thrombosis. J Vasc Surg 2002;35:278–85.

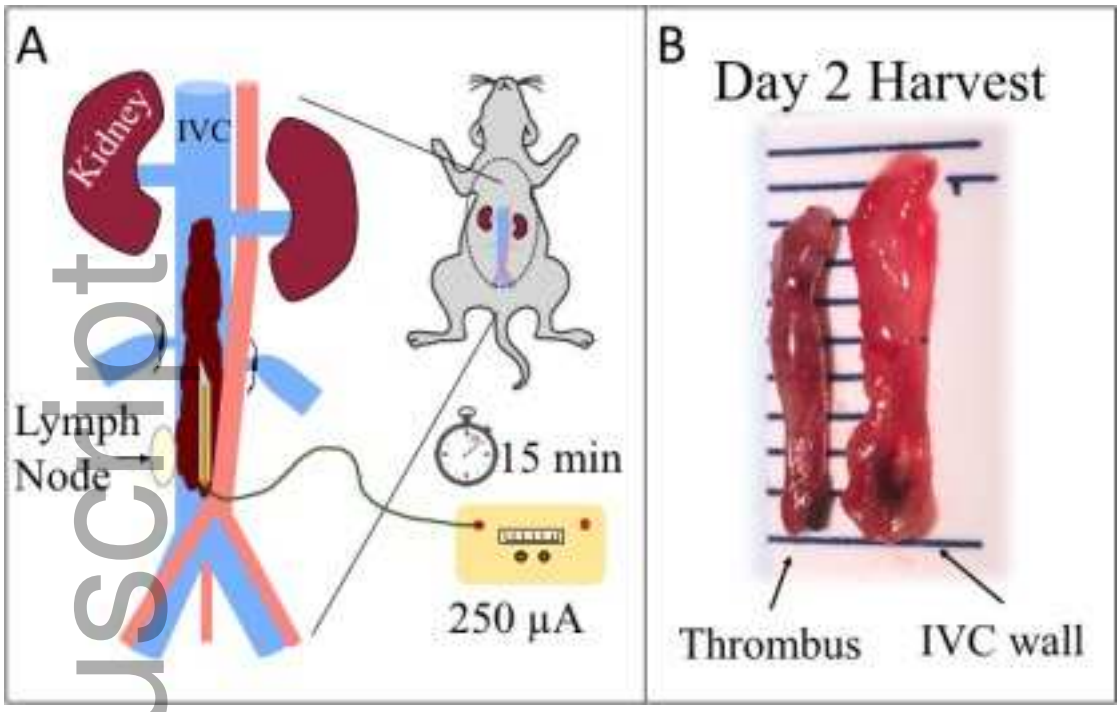

rth2_12074_f1.tiff

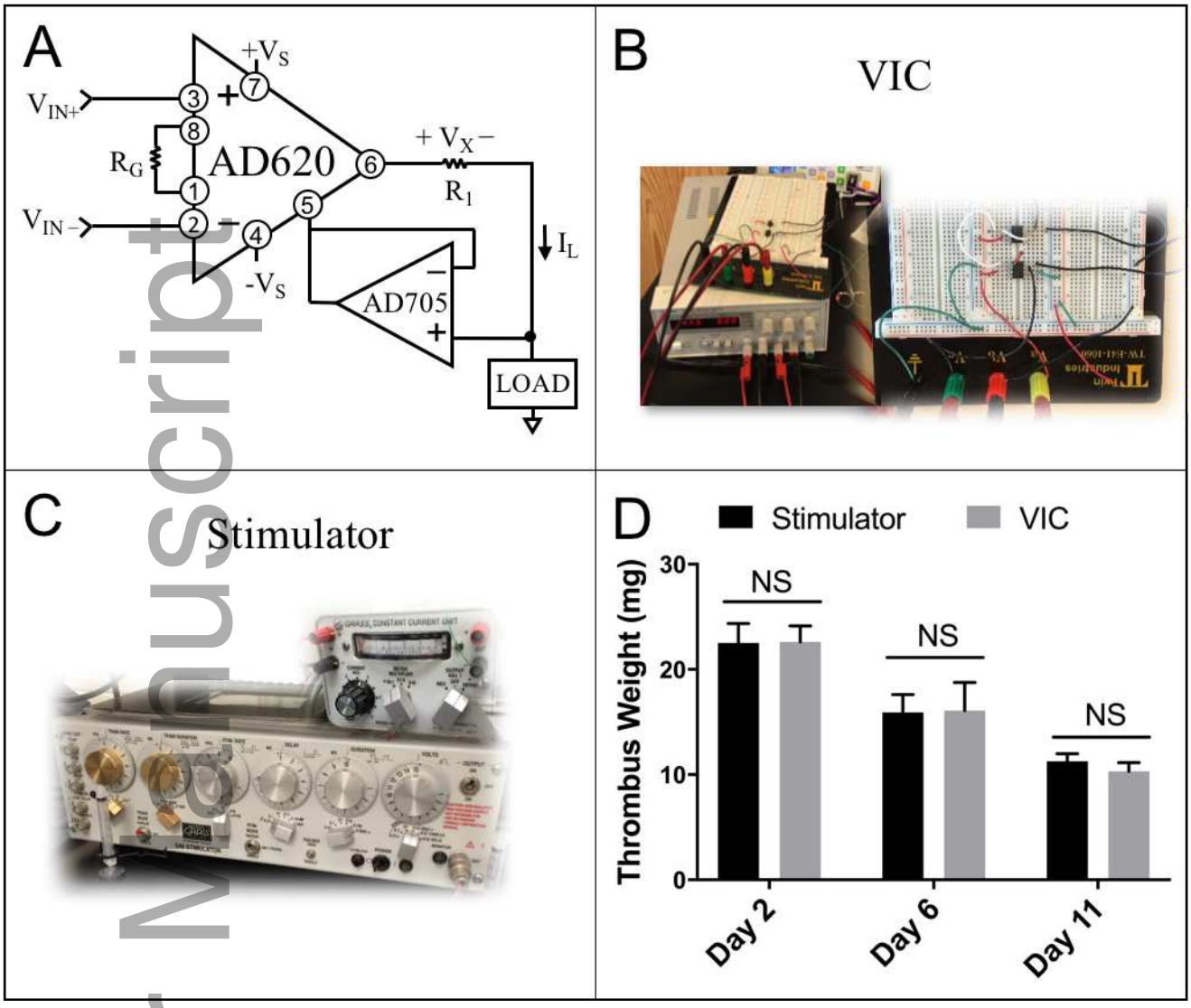

rth2_12074_f2.png

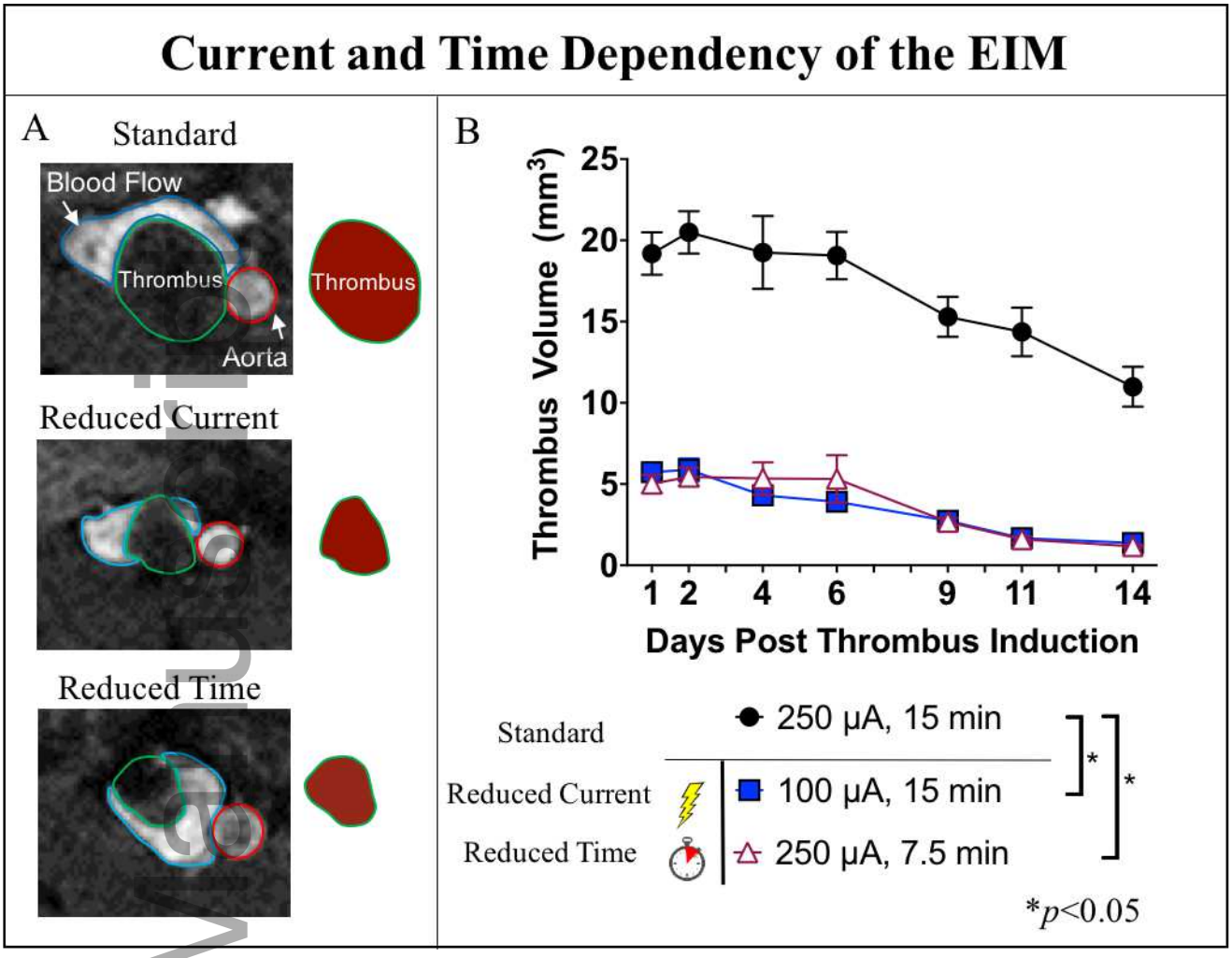

rth2_12074_f3.tiff

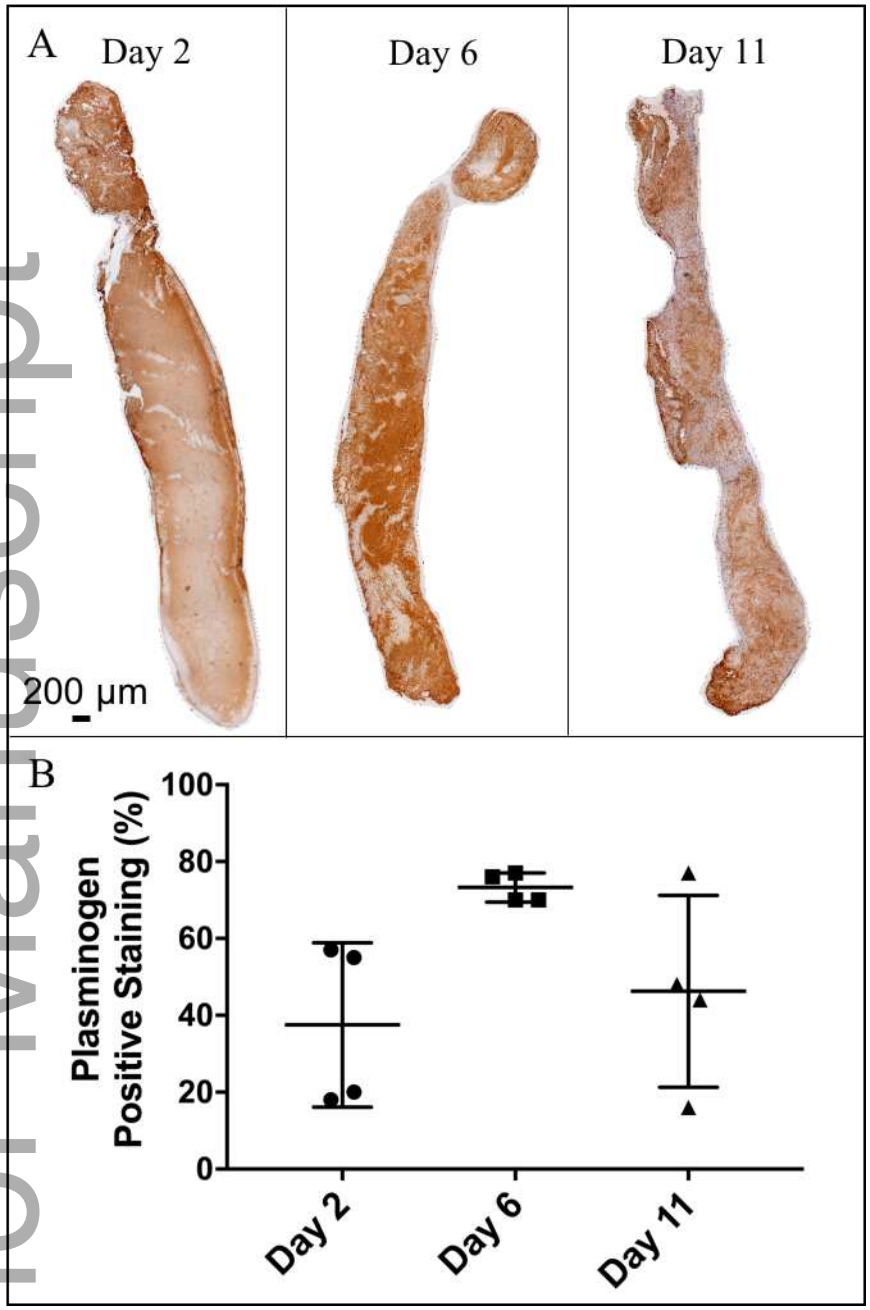

rth2_12074_f4.tiff

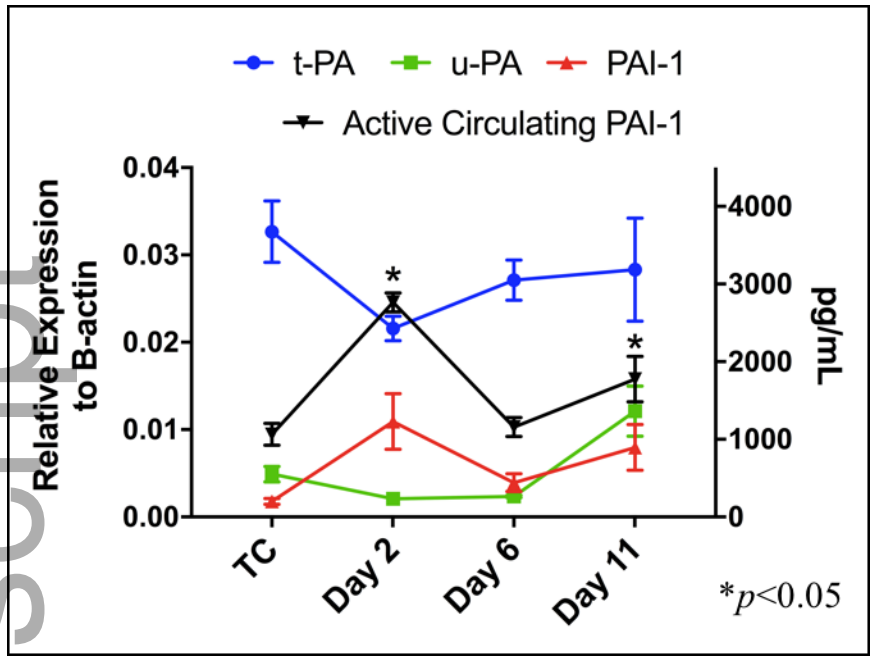

rth2_12074_f5.tiff